15 March 1996

ELSEVIER

Optics Communications 124 (1996) 500–504

OPTICS COMMUNICATIONS

Solitons in fiber amplifiers beyond the parabolic-gain and rate-equation approximations

L.W. Liou, Govind P. Agrawal

The Institute of Optics, University of Rochester, Rochester, NY 14627, USA

Received 21 August 1995; revised version received 30 October 1995; accepted 6 November 1995

Abstract

We explore the existence of solitons in a nonlinear, dispersive, amplifying medium based on a model that makes neither the parabolic-gain approximation nor the rate-equation approximation. Without these approximations, the Maxwell-Bloch equations no longer reduce to a Ginzburg-Landau equation and do not appear to have analytic soliton solutions. We use numerical simulations to show that solitary waves can exist provided there is enough broadband loss such that the net gain is negative far away from the gain peak. In general, such solitons are chirped and the degree of chirp as well as the soliton width depend on the amount of loss.

The propagation of short pulses in optical fibers is governed by the well-known nonlinear Schrödinger equation (NSE) which takes the dispersive and nonlinear effects of the fiber into account [1,2]. Exact solutions of the NSE, called solitons, can be found through the inverse scattering method [3]. Such pulses propagate unchanged over long distances in the absence of loss. However, optical fibers are inherently lossy, and some type of gain mechanism is required to compensate for the loss. A common technique consists of doping the silica fiber with rare-earth ions and pumping them optically to realize the optical gain [4]. By modeling the doped optical fiber as a gain medium with a parabolic gain profile, the solitary-wave solutions of the modified NSE have been obtained [5,6]. This solution shows that for a pulse to propagate undistorted in an amplifying medium, the soliton must be chirped in addition to satisfying a certain relationship between the peak power and the width of the pulse [5,6]. This analytic solution applies to any nonlinear gain medium that can be modeled with a parabolic gain profile. The validity of this model for realistic gain profiles raises many questions, the foremost among them being the artificial introduction of large losses in the spectral wings. Also, the appropriateness of the rate-equation approximation is questionable since the soliton width can become comparable to the dipole relaxation time. In this Letter we use numerical simulations to demonstrate that solitons in fiber amplifiers can exist under certain conditions even when both the rate-equation and parabolic-gain approximations are relaxed.

Numerical simulations for pulse evolution in fiber amplifiers have been performed extensively [7–10]. It was found necessary to use the full Maxwell-Bloch formalism for femtosecond pulses [8–10]. Thus, we model the dopants as a two-level atomic system whose response is governed by the Bloch equations [11]:

$$d\sigma/dt = -(i\Delta + T_2^{-1})\sigma - i\Omega w\,, \quad (1a)$$

$$W_p = -T_1^{-1}(w - w_0) - \mathrm{Im}(\Omega\sigma^*)\,, \quad (1b)$$

where σ is the microscopic polarization, w is the population inversion, W_p is the pump rate, w_0 is the popu-

SSDI 0030-4018(95)00690-7

lation inversion at thermal equilibrium, Δ is the detuning of the optical field from the atomic resonance frequency, T_1 is the population decay time (~ 10 ms for erbium ions), T_2 is the dipole relaxation time (~ 0.1 ps) and $\Omega = \mu E/\hbar$ is the on-resonance Rabi frequency with μ as the dipole moment and E the slowly varying complex amplitude of the electric field.

The dopant-induced gain can be included by adding a source term to the standard NSE [1]. The resulting equation becomes

$$\frac{\partial E}{\partial z} + \frac{1}{v_g}\frac{\partial E}{\partial t} + \frac{i}{2}\beta_2 \frac{\partial^2 E}{\partial t^2} - i\gamma|E|^2 E + \frac{\alpha}{2}E = \frac{i\mu_0\omega_0 c}{2n_0} P_D(t) , \quad (2)$$

where v_g is the group velocity, $\beta_2 = (d^2\beta/d\omega^2)_{\omega=\omega_0}$ is the group-velocity dispersion coefficient with $\beta(\omega) = n(\omega)\omega/c$, $\gamma = n_2\omega_0/c$ is the nonlinearity coefficient, α is the loss coefficient, ω_0 is the optical frequency, n_0 is the value of the refractive index at the frequency ω_0, and μ_0 is the permeability of free space. Assuming predominantly homogeneous broadening of the gain spectrum, the macroscopic polarization is given by $P_D = N\mu\sigma$, where N is the number density of dopants, and σ is obtained from the Bloch equations. The effects of inhomogeneous broadening can be included if necessary.

Erbium-doped fibers have a relatively high saturation energy [12] (~ 10 μJ). For typical pulse energies (<1 nJ), gain saturation is negligible during amplification of a single pulse, and the population inversion of the dopants is expected to remain relatively constant [10] at the value $\bar{w} = w_0 + W_p T_1$. Assuming that the amplifier operates at the gain peak ($\Delta = 0$), Eq. (1a) can be solved in the frequency domain. The result can be used to obtain the susceptibility of the gain medium given by

$$\chi(\omega) = \frac{n_0 c g_0}{\omega_0} \frac{(\omega - \omega_0)T_2 - i}{1 + [(\omega - \omega_0)T_2]^2} , \quad (3)$$

where g_0 is the small-signal gain coefficient. By using $\tilde{P}_D(z,\omega) = \epsilon_0 \chi(\omega)\tilde{E}(z,\omega)$, where a tilde denotes the Fourier transform, together with Eq. (3), Eq. (2) can be written as a generalized NSE:

$$\frac{\partial E}{\partial z} + \frac{1}{v_g}\frac{\partial E}{\partial t} + \frac{i}{2}\beta_2 \frac{\partial^2 E}{\partial t^2} - i\gamma|E|^2 E + \frac{\alpha}{2}E = \frac{\omega_0}{2n_0 c}\frac{1}{2\pi}\int_{-\infty}^{\infty} \chi(\omega)\, \tilde{E}(z,\omega)\, \exp(-i\omega t)\, d\omega . \quad (4)$$

It is important to note that the rate-equation approximation is not made in obtaining Eq. (4) so that this equation is valid even for pulses of widths shorter than T_2. Eq. (4) includes the dopant-induced dispersion of both the gain and the refractive index. Under the homogeneous broadening assumption made in Eq. (3), the gain spectrum is Lorentzian.

In the parabolic-gain approximation, the complex susceptibility is expanded in a Taylor series around the carrier frequency ω_0 up to the quadratic term. This results in a modified NSE which can be rewritten in a normalized form [1,7].

$$i\frac{\partial u}{\partial \xi} - \tfrac{1}{2}(s + id)\frac{\partial^2 u}{\partial \tau^2} + |u|^2 u = \frac{i}{2}\mu u , \quad (5)$$

where $\xi = z/L_D$, with the dispersion length $L_D = T_2^2/|\beta_2|$, $\tau = (t - z/v_g)/T_2$ is the normalized time, $s = \mathrm{sgn}(\beta_2) = \pm 1$, $d = g_0 L_D$ which is related to the curvature of the gain profile at the gain peak, and $\mu = (g_0 - \alpha)L_D$ is the net gain. Eq. (5) is in the form of a Ginzburg-Landau equation that has been well studied in different fields [13]. Despite the fact that the loss and gain make it a non-conservative system, Eq. (5) is known to have a chirped solitary-wave solution given by [1,5]

$$u(\xi,\tau) = N[\mathrm{sech}(p\tau)]^{(1+iq)} \exp(i\Gamma\xi) , \quad (6)$$

where the soliton amplitude N, width parameter p, chirp parameter q, and propagation constant Γ must satisfy certain relationships as given in Ref. [1]. This parabolic-gain model supports gain-guided chirped solitons in both the normal and anomalous dispersion regimes.

It is not clear whether the generalized NSE in Eq. (4) obtained without making the rate-equation and parabolic-gain approximations will support a solitary wave since, unlike with the parabolic-gain approximation where a large amount of loss is artificially introduced in the spectral wings, some gain exists at all frequencies. However, this situation can be remedied in practice by requiring the fiber amplifier to have a certain amount of broadband loss to counter the gain in the spectral wings of the pulse (net loss) while the central part of the pulse spectrum experiences net gain.

To study whether solitary waves exist under such conditions, Eq. (4) is solved numerically by using a split-step algorithm [1]. The chirped soliton given in Eq. (6) is taken as the input pulse shape after choosing $T_2 = 0.2$ ps. Fig. 1 shows the evolution of the pulse in the anomalous-dispersion region of a distributed-gain fiber amplifier out to 40 dispersion lengths. Fig. 1a corresponds to $\alpha/g_0 = 0.6$, and Fig. 1b corresponds to $\alpha/g_0 = 0.8$. In Fig. 1a, the shape of the input pulse, or the parabolic-gain soliton (PGS), evolves into a steady-state pulse which is narrower and has a higher peak power than the PGS. In contrast, Fig. 1b shows that the PGS evolves into a wider pulse having a smaller peak power. In both cases a steady-state appears to have been reached, despite a slight shifting of the pulse in the time domain which is due to the dopant-induced index dispersion mentioned earlier.

Extensive numerical simulations show that a steady-state is reached over a wide range of $\alpha/g_0 \approx 0.4$–0.9, but the pulse shapes are significantly different except for $\alpha/g_0 \approx 2/3$ for which the external loss roughly equals the artificial loss introduced by the parabolic-gain approximation. This means that the Maxwell-Bloch model of the fiber amplifier does indeed have solitary-wave solutions. However, the stability of such solutions is not guaranteed and may depend on the operating parameters. For example, the soliton for the case of $\alpha/g_0 = 0.6$ in Fig. 1a remains stable to distances as long as 80 dispersion lengths while the soliton in Fig. 1b for $\alpha/g_0 = 0.8$ shows some signs of instability around 30 dispersion lengths.

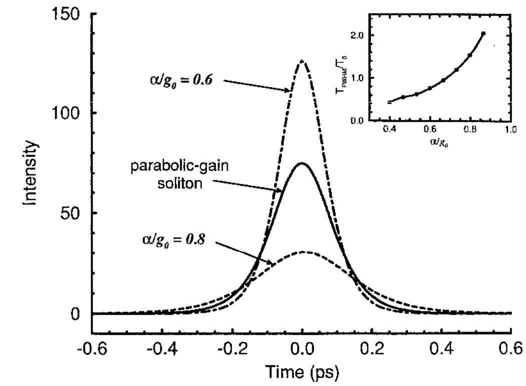

Fig. 2. Comparison of the steady-state soliton shapes of Fig. 1 for $\alpha/g_0 = 0.6$ and 0.8 with the parabolic-gain soliton (solid curve) for which $\alpha = 0$. Inset shows the steady-state pulse width (normalized to the PGS soliton width) as a function of α/g_0.

Fig. 2 shows a comparison of the PGS (solid curve), obtained under identical conditions except for $\alpha = 0$, with the final steady-state pulses of Fig. 1 (dashed curves). Pulse spectra are not shown since their shapes are similar except for their widths. The pulse width of the soliton varies with the ratio α/g_0 as shown in the inset of Fig. 2. In general, the soliton becomes narrower as α/g_0 decreases. This is because the higher net gain causes pulse compression. Outside the range of values shown for α/g_0, steady-state pulses were not seen. This

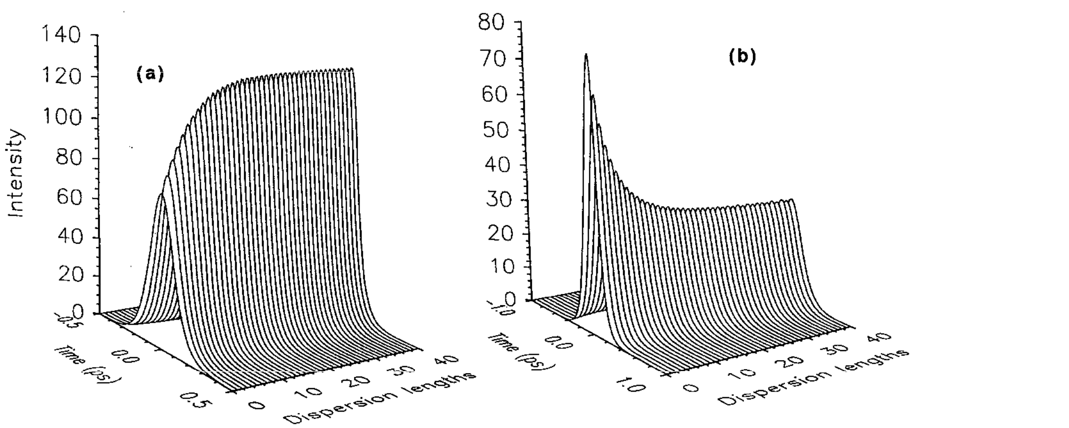

Fig. 1. Evolution toward the steady-state soliton over 40 dispersion lengths for (a) $\alpha/g_0 = 0.6$ and (b) $\alpha/g_0 = 0.8$ in a distributed fiber amplifier having 3 dB gain per dispersion length. The input pulse corresponds to the parabolic-gain soliton.

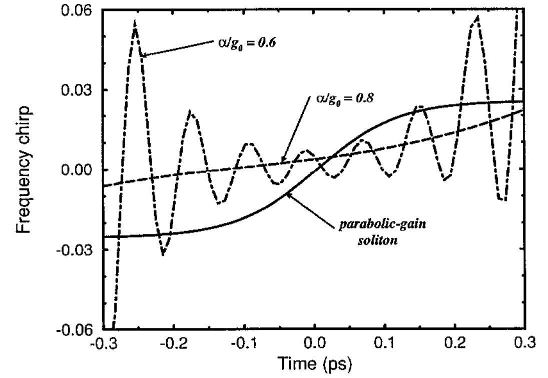

Fig. 3. Frequency chirp profiles for the three solitons shown in Fig. 2.

can be understood for the case of small losses by noting that so much energy is shed as dispersive waves that a steady-state pulse is never formed. In the other extreme of large losses, there is not enough gain to overcome the dispersion of the fiber. Note that it is the ratio α/g_0 that determines the final pulse width in the steady state, not the actual values of the gain and loss. In the PGS case, external loss is not necessary since loss is artificially introduced in the spectral wings.

The most significant difference between the PGS solution of Eq. (6) and the solitary-wave solutions obtained from the Maxwell-Bloch model is the chirp imposed across the soliton. This change is important since it is the frequency chirp that allows the PGS to exist in the parabolic-gain model. Fig. 3 compares the frequency chirp for the three solitons seen in Fig. 2. The solid curve corresponds to the PGS. For large losses ($\alpha/g_0 \gtrsim 0.7$), the chirp is nearly zero across the center of the pulse. However, as α/g_0 decreases, the amount of chirp imposed on the soliton increases in an oscillatory manner. The physical reason behind chirp oscillations is not clear at present.

The results shown in Figs. 1–3 correspond to a fixed value of g_0 given by $\exp(g_0 L_D) = 2$. For moderate values of g_0, the final pulse characteristics are virtually identical with those shown in Figs. 1–3; the important parameter is the ratio α/g_0 as mentioned earlier. However, for much larger values of net gain, the qualitative behavior may change significantly. For example, for a net gain of 10 dB per dispersion length, the input pulse quickly compresses and then begins to split into multiple subpulses. This behavior is similar to that of Ref. [7] where the parabolic-gain approximation was used in the model. One major difference is that the subpulses are narrower in this case (pulse width $< T_2$) which is allowed since the rate-equation approximation was not used in this model. This feature also suggests that fiber amplifiers can be used to simultaneously amplify and compress optical pulses down to about 100 fs. For these ultrashort pulse widths, higher order nonlinear effects which were not included in this model may effect the final pulse characteristics as well.

It is interesting to point out that the parabolic-gain model predicts the existence of a PGS even in the normal-dispersion region [5], whereas solitons do not exist in this regime in undoped fibers. Thus, the question arises as to whether the model given in Eq. (4) can support a solitary wave in the normal dispersion regime. Numerical simulations were carried out under the same conditions as for Fig. 1 except in the normal dispersion regime. The input PGS was seen to disperse rapidly and then to break-up into subpulses. The reason for this behavior is that the chirp imposed across the pulse in the normal dispersion regime is quite large compared to the chirp acquired by the pulse in the anomalous dispersion regime. This large chirp combined with the dopant-induced index dispersion prevents the pulse from approaching the steady-state. Fig. 4 shows the pulse shape and spectrum for a pulse after it has propagated 10 and 12 dispersion lengths in the amplifier. The loss α is set to 4.5 dB/L_D, and g_0 is set to 7.5 dB/L_D, yielding a ratio of α/g_0 of 0.6. It is seen that the pulse width is fairly wide (26 ps, FWHM). The chirp (not shown) also has a hyperbolic tangent

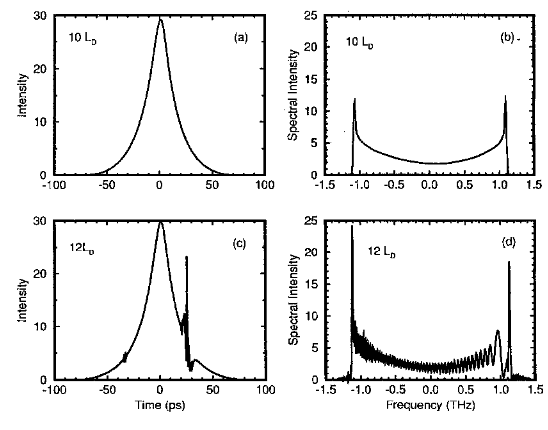

Fig. 4. Comparison of pulse characteristics for pulse propagating in the normal dispersion regime for $\alpha/g_0 = 0.6$; (a) pulse shape at $10L_D$, (b) spectrum at 10 L_D, (c) pulse shape at 12 L_D, (d) spectrum at 12 L_D.

profile with a maximum nearly two orders of magnitude greater than the chirp imposed on the pulse in the anomalous dispersion regime shown in Fig. 3. The shape and spectrum (Fig. 4a and 4b) are very smooth up to 10 L_D, but soon afterwards the pulse begins exhibiting signs of instability. Fig. 4d shows a fast ripple across the spectrum at 12 L_D and manifests itself as a distortion of the pulse shape which leads to the eventual break-up of the pulse.

To verify the impact of the dopant-induced dispersion on the stability of propagating pulses, this effect was removed from the model and the simulations were repeated. Under this restriction, a steady-state was indeed found, as reported in Ref. [7]. This leads to the conclusion that the large chirp imposed on the pulse in the normal dispersion regime in combination with the dopant-induced dispersion prevents the development of a steady-state solution.

Finally, in the case of a distributed fiber amplifier (operating in the anomalous dispersion regime), where the fiber is lightly doped over the entire length so as to just compensate the loss of the fiber (~0.2 dB/km), the required small-signal gain would be quite small, on the order of $\exp(g_0 L_D) = 1.07$. This would minimize the amount of reshaping that the pulse undergoes as it attempts to reach a steady state, and thus also minimizes the dispersive waves shed in the process, in contrast with the traditional lumped fiber amplifiers. In addition, special filters may be placed in the system to control the pulse width to prevent higher-order effects such as third-order dispersion and intrapulse stimulated Raman scattering from playing an important role in the evolution of the pulse. Results for a distributed fiber amplifier system will be discussed in a future publication.

In conclusion, the results of numerical simulations based on Maxwell-Bloch equations [Eq. (4)] show that solitary waves can exist even when the parabolic-gain and rate-equation approximations are not made. However, in contrast with the parabolic-gain model, such solitons exist only in the anomalous-dispersion region. The characteristics of the chirp imposed across the pulse depends on the amount of losses in the system relative to the amplifier gain, and the final pulse width of the soliton can also be changed by controlling the amount of loss.

This research is supported in part by the U.S. Army Research Office. L.W. Liou acknowledges support from the U.S. Department of Education for a graduate fellowship.

References

[1] G.P. Agrawal, Nonlinear Fiber Optics, 2nd Ed. (Academic, New York, 1995).
[2] A. Hasegawa, Optical Solitons (Springer-Verlag, New York, 1989).
[3] V.E. Zakharov and A.B. Shabat, Sov. Phys. JETP 34 (1972) 62.
[4] E. Desurvire, Erbium-doped Fiber Amplifiers (Wiley, New York, 1994).
[5] P.A. Bélanger, L. Gagnon and C. Paré, Optics Lett. 14 (1989) 943.
[6] N.N. Pereira and L. Stenflo, Phys. Fluids 20 (1977) 1733.
[7] G.P. Agrawal, Phys. Rev. A 44 (1991) 7493.
[8] B. Gross and J.T. Manassah, Optics Lett. 17 (1992) 340.
[9] V.V. Afanasjev, V.N. Serkin, V.A. Vysloukh, Sov. Lightwave Commun. 2 (1992) 35.
[10] S. Chi, C.W. Chang and S. Wen, Optics Comm. 106 (1994) 193.
[11] L. Allen and J.H. Eberly, Optical Resonance and Two-Level Atoms (Dover, New York, 1975).
[12] G.P. Agrawal, Optics Lett. 2 (1990) 875.
[13] R.J. Deissler, J. Stat. Phys. 54 (1989) 1459.